All-optical simultaneous amplitude and phase regeneration for MPSK signal with ASE noise based on two-wave PSA

Hong Liu[a,b], Hongxiang Wang[a], Ganapathy Senthil Murugan[b], Yuefeng Ji[a,*]

[a] *The State Key Laboratory of Information Photonics and Optical Communications, School of Information and Communication Engineering, Beijing University of Posts and Telecommunications, Beijing 100876, China*
[b] *Optoelectronics Research Centre, University of Southampton, Southampton SO17 1BJ, UK*

Abstract

A phase sensitive amplification (PSA) regeneration model for M-ary phase shift keying (MPSK) signals with amplified spontaneous emission (ASE) noise based on the interference between signal and its (M+1)th harmonic is proposed. Compared with the existing models based on different combinations of signal and harmonics, the new regeneration model is optimal in theory to deal with the MPSK signal degraded by ASE noise. The QPSK format is taken as an example for simulation verification and two existing classic models are also performed with the same parameters for comparison. The regeneration performance is evaluated by input-output constellations, phase and amplitude regeneration factors, and the relay distance at the bit error rate (BER) of 3.8×10^{-3} by measuring the transmission reach after the regenerator. The results show that the new model has the optimal relay performance for ASE-noise MPSK format, which is promising to be applied in large-capacity, flexible, and reliable optical transport networks.

Keywords: Phase sensitive amplification, MPSK signal, Simultaneous amplitude and phase regeneration, Two-wave model, ASE noise

*Corresponding author
Email address: jyf@bupt.edu.cn (Yuefeng Ji)

1. Introduction

With the advent of the fifth generation (5G) mobile communications era, large-capacity, low-latency, and high-efficiency flexible optical transport network is playing a crucial role in modern fiber communications [1]. The optical information processing techniques driven by artificial intelligence in optical communication devices and network are ones of the important directions for future development [2], and diverse modulation formats with simple implement or high spectral efficiency (SE) are employed widely on demand. Among these mainstream modulation formats, M-ary phase shift keying (MPSK) format is quite popular because of its higher SE than on-off keying (OOK) and better fiber nonlinear tolerance than quadrature amplitude modulation (QAM) [3]. However, such high-order modulation format is more sensitive to phase noise, which poses a key limitation in both transmission reach and communication capacity.

Several all-optical signal regeneration technologies, which can break the electronic rate bottleneck and support in-line signal processing [4], have been widely studied to increase transmission reach. They are phase-conjugated twin waves (PCTW), optical phase conjugation (OPC), and phase sensitive amplification (PSA). PCTW can mitigate nonlinear distortions of signal by transmitting a pair of phase-conjugated optical signals together at two orthogonal polarizations [5] or two different wavelengths [6], and then coherently superimposing them at the receiver. This method is not only modulation format insensitive but wavelength transparent, which is desirable to regenerate wavelength division multiplexing (WDM) signals. However, it reduces the total transmission capacity by half. Additional electronic hardware is required to double its SE at the expense of extra crosstalk [7]. OPC is a more preferred way to avoid such inefficient use of the spectral bandwidth by lumped midlink spectral inversion [8, 9]. The nonlinear signal impairments accumulated in the first half of the fiber can be compensated by subsequently propagating its conjugated signal in the remaining half of the fiber. However, such a position-sensitive method is only effective for point-to-point transmission links but not flexible routing opti-

cal networks [10]. Different from them, PSA is used to mitigate both linear and nonlinear impairments of MPSK signals by unique phase squeezing characteristic. It is inherently a single-wavelength technology but can also regenerate the WDM signals with the help of optical time lenses [11], which can perform an optical conversion between the WDM channels and the time division multiplexing (TDM) channels. In particular, it can avoid the halved-SE problem and is rather suitable for flexible optical networks.

PSA-based regeneration technology has been widely employed for BPSK [12], QPSK [13–20], 8PSK formats [21] and even for 8QAM [22, 23]. Nevertheless, it has an inherent drawback that it converts phase noise to amplitude noise, and the latter may be converted back into phase noise by the nonlinear effect in transmission, which will seriously affect the transmission reach. To solve this problem, some schemes opt to add additional amplitude regeneration setups after PSA setup, such as parametric saturation [17, 18] or nonlinear optical loop mirror (NOLM) [20, 21]. However, due to the unfriendly nature of PSA to amplitude in the first stage and limited flat area for amplitude regeneration in the second stage, such methods are not only complicated but also have limited ability in dealing with ASE noise. Some schemes opt to realize the simultaneous phase and amplitude regeneration in a single PSA-based NOLM [22, 23]. However, the mechanisms of phase and amplitude regeneration still remain independent essentially so that these schemes are often difficult in its optimization along with compromised regeneration performance. To realize a truly complete regeneration in theory, some schemes opt to modify the traditional two-wave model as three-wave model to suppress the phase-dependent amplitude noise conversion [14–16]. However, this technology only focuses on the regeneration of MPSK signal with pure phase noise. Although ASE noise is necessarily realistic representations of noise in fiber communications, to the best of our knowledge, there is no theoretical PSA regeneration model targeted at ASE-noise MPSK signals.

In this paper, we study an optimal regeneration model for ASE-noise MPSK formats based on two-wave PSA. By analyzing a complete PSA model of three-

wave interference, it is proved theoretically that the optimal model could be still a simple two-wave interference but realized by the signal and its (M+1)th harmonic. The regeneration characteristics of the new model are analyzed and compared with another two existing classical models. QPSK signal (M=4) is taken as an example for verification. The system performance can be evaluated by the input-output constellations and the calculated phase and amplitude regeneration factors under different optical signal-to-noise ratio (OSNR). Finally, to assess the system relay performance, the transmission reach after the regenerator is measured corresponding to the bit error rate (BER) of 3.8×10^{-3}. Compared with existing models, our new two-wave model evidences a more excellent ability in reachable transmission distance after regeneration.

2. Operation principle

2.1. Optimal PSA-based Regeneration Model

The key for MPSK signal regeneration based on PSA is to obtain the phase squeezing axis $\varphi = 2n\pi/M$ $(n = 1, 2, ..., M)$, M is the order of modulation. In the traditional model, it is realized by the interference between signal $e^{j\varphi_s}$ and its conjugated harmonic $e^{-j(M-1)\varphi_s}$. Actually, the other interference between signal $e^{j\varphi_s}$ and its harmonic $e^{j(M+1)\varphi_s}$ should also be feasible to enable such function. Therefore, the three-wave interference model should be the complete model to study MPSK signal regeneration, which can be expressed as:

$$A_{out}e^{j\varphi_{out}} = A_s e^{j\varphi_s} + m(A_s e^{-j\varphi_s})^{M-1} + n(A_s e^{j\varphi_s})^{M+1}, \tag{1}$$

where A and φ represent the signal amplitude and phase respectively, m and n are the amplitude ratio of the corresponding harmonic to signal respectively. In practice, the harmonics are generated by the signal so that $|m| < 1$ and $|n| < 1$.

As for the input MPSK signal with ASE noise, it can be expressed as:

$$A_s e^{j\varphi_s} = e^{j\varphi_m} + A_n e^{j\varphi_n}, \tag{2}$$

where φ_m is the modulated phase information $2n\pi/M$ $(n = 1, 2, ..., M)$. The MPSK signal has a normalized amplitude. A_n represents the amplitude noise

and obeys normal distribution. φ_n is a random value uniformly distributed in the interval $(0, 2\pi)$. The ASE noise can be added directly to MPSK signal by an OSNR module in simulation. The relationship between OSNR and A_n is:

$$OSNR = 10\log_{10}\frac{P_s}{P_n} = 10\log_{10}\frac{\sum_{i=1}^{N}|1|^2}{\sum_{i=1}^{N}|A_{n,\,i}|^2}, \tag{3}$$

where P_s and P_n are signal power and noise power respectively. N is the symbol length of the signal data and set as $2^{13} = 8192$. $A_{n,\,i}$ represents the received noise amplitude.

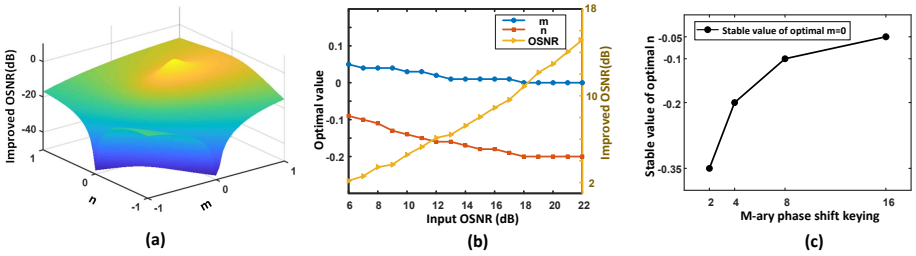

Figure 1: (a) Improved OSNR for input 20dB QPSK with different m and n; (b) Best regeneration performance and the corresponding optimal value of m and n under different input quality; (c) Stable values of optimal m and n for different MPSK formats.

Here we take the QPSK (M=4) format as an example to study the optimal m and n. The OSNR difference between the input and output signals serves as an indicator for the assessment of regeneration performance. According to Eq. (1) and Eq. (2), when the QPSK signal is input with 20dB OSNR, the improved OSNR of output signal varies significantly with different m and n as shown in Fig. 1(a). Most importantly, there is only one best regeneration peak, which corresponds to the optimal m and n. Similarly, given different input quality of QPSK, the optimal m and n values for best regeneration performance can also be found and given in Fig. 1(b). It can be observed that the optimal m and n are close to 0 and -0.2, respectively under the case of lower signal quality and stable at 0 and -0.2 at the higher signal quality. Based on the same analysis method, such characteristic of optimal m and n that are close and tend to be at a stable value respectively can also be found in other MPSK formats. As shown

in Fig. 1(c), the stable values of optimal m and n are 0 and about $-1/(M+1)$ respectively. In practice, the values of m and n should be determined for a certain system. Therefore, the two stable values are chosen as the optimal regeneration parameters, and the optimal regeneration model for MPSK signal with ASE noise can be expressed as:

$$A_{out}e^{j\varphi_{out}} = A_s e^{j\varphi_s} - 1/(M+1)(A_s e^{j\varphi_s})^{M+1}. \tag{4}$$

Different with the traditional model, it is realized by the interference between signal $e^{j\varphi_s}$ and its harmonic $e^{j((M+1)\varphi_s+\pi)}$.

2.2. Comparison Of Regeneration Characteristics

In order to illustrate the optimal characteristics of the new model in dealing with ASE noise, the regeneration characteristics of the traditional two-wave model and the three-wave model are also analyzed and compared for reference.

For the traditional model [13], according to the input signal in Eq. (2), the regenerated signal can be expressed as:

$$A_{out1}e^{j\varphi_{out1}} = e^{j\varphi_m} + A_n e^{j\varphi_n} + 1/(M-1)(e^{-j\varphi_m} + A_n e^{-j\varphi_n})^{M-1}. \tag{5}$$

By binomial theorem, the (M-1)th harmonic in Eq. (5) can be expanded into series as:

$$\begin{aligned}&\binom{M-1}{0}/(M-1)\times e^{-j(M-1)\varphi_m} + \binom{M-1}{1}/(M-1)A_n \times e^{-j\varphi_n}e^{-j(M-2)\varphi_m} \\ &+ ... + \binom{M-1}{M-1}/(M-1){A_n}^{M-1} \times e^{-j(M-1)\varphi_n},\end{aligned} \tag{6}$$

where the first item represents the pure MPSK signal due to $M\varphi_m = 2\pi$, and the other items are induced noise with a weight of $\binom{M-1}{k}/(M-1){A_n}^k$ $(k = 1, 2, ..., M-1)$ respectively. Among them, the first noise item $A_n \times e^{-j\varphi_n}e^{-j(M-2)\varphi_m}$ plays a major role in all noise items since $A_n \ll 1$. It can totally transfer the

original ASE noise $A_n e^{j\varphi_n}$ in Eq. (5) to the pure amplitude noise:

$$\begin{aligned} & A_n e^{j\varphi_n} + A_n \times e^{-j\varphi_n} e^{-j(M-2)\varphi_m} \\ =& A_n \times [cos\varphi_n + cos\,(2\varphi_m - \varphi_n) + j \times [sin\varphi_n + sin\,(2\varphi_m - \varphi_n)]] \\ =& A_n \times [2cos\varphi_m cos\,(\varphi_m - \varphi_n) + 2j \times sin\varphi_m cos\,(\varphi_m - \varphi_n)] \\ =& 2A_n cos\,(\varphi_m - \varphi_n)\,[cos\varphi_m + j \times sin\varphi_m] \end{aligned} \tag{7}$$

Therefore, the traditional model has the characteristic of phase-dependent amplitude noise conversion.

As for the new model, the regenerated signal can be obtained as:

$$A_{out2} e^{j\varphi_{out2}} = e^{j\varphi_m} + A_n e^{j\varphi_n} - 1/(M+1)(e^{j\varphi_m} + A_n e^{j\varphi_n})^{M+1}. \tag{8}$$

and (M+1)th harmonic can be expanded as:

$$\begin{aligned} & -\binom{M+1}{0}/(M+1) \times e^{j(M+1)\varphi_m} - \binom{M+1}{1}/(M+1) A_n \times e^{j\varphi_n} e^{jM\varphi_m} \\ & - ... - \binom{M+1}{M+1}/(M+1) {A_n}^{M+1} \times e^{j(M+1)\varphi_n}, \end{aligned} \tag{9}$$

Similarly, the first item is the signal and the other items are induced noise with the weight of $\binom{M+1}{k}/(M+1){A_n}^k$ $(k = 1, 2, ..., M+1)$ respectively. Obviously, the original noise of the signal $A_n e^{j\varphi_n}$ in Eq. (5) can be directly eliminated by the first noise item $-A_n \times e^{j\varphi_n} e^{jM\varphi_m}$ in harmonic. In this way, a simultaneous and comparable regeneration ability both on phase and amplitude for MPSK signal with ASE noise is realized.

Theoretically, when the A_n is smaller, the first noise item will have a bigger weight in all noise items, and then the regeneration characteristic of new model will be more obvious. Therefore, the OSNR thresholds of input MPSK signals that can be regenerated are further studied. For regeneration, the input OSNR should be smaller than the output OSNR, so it satisfies:

$$\frac{\sum_{i=1}^{N} |1|^2}{\sum_{i=1}^{N} |A_{n,\,i}|^2} < \frac{\sum_{i=1}^{N} \left|\frac{M}{M+1}\right|^2}{\sum_{k=2}^{M+1} \sum_{i=1}^{N} \left| \binom{M+1}{k} / (M+1) \times A_{n,i}^k \right|^2} \tag{10}$$

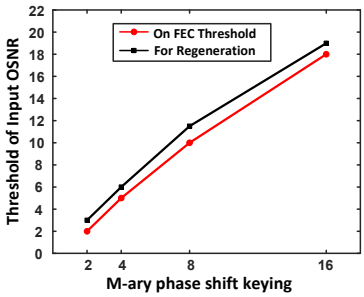

Figure 2: The OSNR threshold for the regeneration of different MPSK formats in new model.

The numerical solution for each MPSK format is shown in Fig. 2. For reference, the threshold of OSNR corresponding to the forward error correction (FEC) threshold of 3.8×10^{-3} is also given [24]. Fig. 2 shows that the new model has a strong regeneration ability since the OSNR threshold for regeneration is very comparable with the OSNR on the FEC threshold.

Finally, the existing three-wave interference model using both (M+1)th and (M-1)th harmonics can be considered as a combination of the traditional and new models. Compared with the new model, the addition of (M-1)th harmonic might be able to eliminate part of noise in (M+1)th harmonic because of its opposite sign with (M+1)th harmonic as shown in Eq. (6) and Eq. (9). However, the main function of (M-1)th harmonic is converting phase noise to amplitude noise, since the first noise item generally has a bigger weight than the remaining noise items. As such noise conversion is actually an ineffective regeneration for ASE noise, there is no benefit to introduce (M-1)th. Therefore, consistent with the theoretical results, the two-wave model with (M+1)th is the optimal model to deal with the signal degraded by ASE noise.

3. Setup

Fig. 3(a) shows the whole regeneration setup applied for MPSK signals. Here the QPSK format is employed as an example to verify the regeneration characteristics of the new model.

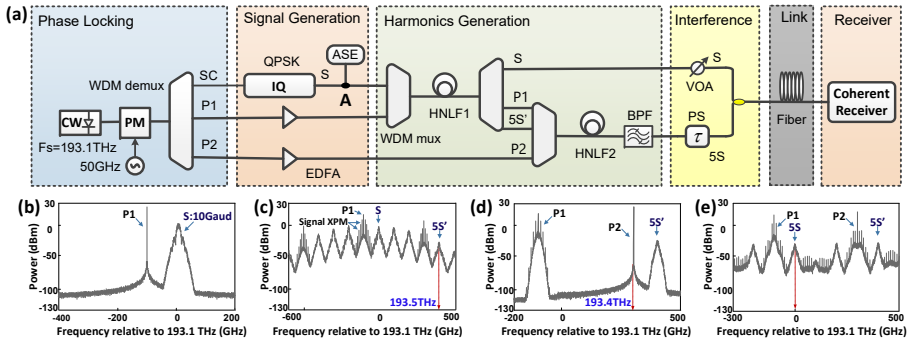

Figure 3: (a) Simulation setup; (b) and (c) are the spectrums before and after HNLF1 respectively; (d) and (e) are the spectrums before and after HNLF2 respectively.

To ensure a stable phase squeezing axis in the final interference stage, a phase modulator (PM) is used at the beginning to modulate a continuous wave (CW) laser with 5KHz linewidth to produce the phase-locked signal carrier (SC) and two pump waves P1 and P2 at the frequency of 193.1THz, 193.0THz and 193.4THz respectively. A 20-Gbps QPSK signal is generated by modulating the SC in an IQ modulator with $2^{15}-1$ pseudo-random binary sequence (PRBS). Different OSNRs of input signal are set at node A. In the harmonics generation stage, 23dBm QPSK and 26dBm P1 are first sent to high nonlinear fiber (HNLF1) to obtain the fifth harmonic 5S' at 193.5THz by four-wave mixing (FWM). The HNLF1 has a nonlinear coefficient $\gamma = 13.1w^{-1}/km$, length L=300m, and zero-dispersion frequency at 193.1 THz with its slope of $0.08ps/nm^2/km$. The optical spectra before and after the HNLF1 are shown in Figs. 3(b) and 3(c) respectively. In Fig. 3(c), the 5th harmonic (-1.6dBm) is generated at 193.5THz with a conversion efficiency of -21dB. The conversion efficiency here is defined as the optical power ratio between the generated harmonic and the original signal. Some spikes in the pump are generated by the cross-phase modulation (XPM) effect with signal.

Then 26dBm P2 with filtered P1 and 5S' is launched into the HNLF2 to generate the 5S at 193.1 THz by FWM , which is then filtered by the bandpass filter (BPF) with a 3-dB bandwidth of 0.32 nm. HNLF2 has the same param-

eters as HNLF1. The optical spectra before and after the HNLF2 are given in Figs. 3(d) and 3(e) respectively. As shown in Fig. 3(e), the 5th harmonic (-1.7dBm) is generated at 193.1THz with a high conversion efficiency of -0.1dB benefited from the two-pump structure. In the interference stage, a variable optical attenuator (VOA) is set as 8dB to adjust the power ratio of the signal S to harmonic 5S as 25:1 ($(M+1)^2 : 1$)). The phase shifter (PS) introduces a static phase compensation to the harmonic for the desirable phase difference π between signal S and harmonic 5S. For such a phase-sensitive setup in practice, an active phase-locking loop is usually employed in the interference stage to stabilize their phase locking relationship, since the three phase-locked waves from optical comb are subsequently processed in different paths [13]. Besides the method of optical comb in our setup, the phase locking relationship can also be obtained by injecting locking the fourth harmonic generated by the signal and P1 as P2 [25]. Further, in practice the high-power P1 and P2 could be phase modulated with 4.5GHz PRBS ($2^{15}-1$) data to suppress the stimulated Brillouin scattering in HNLFs [17].

It needs to be noticed that there is about 10dB loss associated to the regeneration setup, which is mainly caused by the low nonlinearity of HNLF. Such setup loss could be improved by employing high nonlinear integrated device such as on-chip semiconductor optical amplifier (SOA) [26]. Finally, the transmission fiber is added before the receiver to evaluate the system relay performance, the launched signal power to the transmission fiber keeps at 13dBm. The fiber has a loss of $0.2dB/km$, dispersion of $1.6e^{-5}s/m^2$ at 193.1 THz with its slope of $0.08ps/nm^2/km$, and nonlinear coefficient $\gamma = 1.3w^{-1}/km$. The traditional model is also demonstrated based on the same setup for comparison, only by adjusting the harmonics generation stage for conjugated third harmonic at the signal frequency and the interference stage for the power ratio as 9:1($(M-1)^2 : 1$). Moreover, the three-wave model using both (M+1)th and (M-1)th harmonics with the same power ratio $1 : (0.14)^2$ in [16] is also performed by expanding the number of the harmonic generation stage into two, which helps to provide a three-wave interference in the final interference stage.

4. Results and Discussion

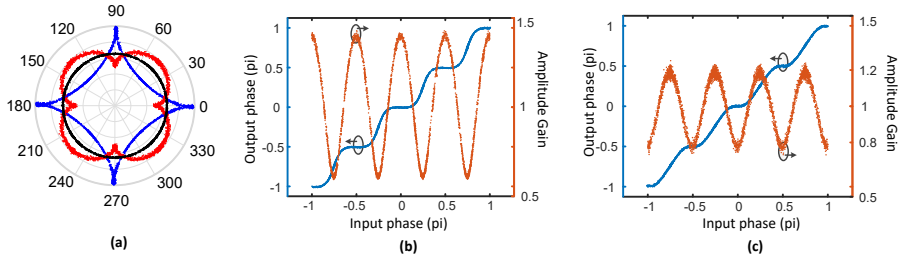

Figure 4: (a) Constellations with all-phase input signal (black) and output signal in traditional two-wave model (blue) and new model (red); (b) and (c) are corresponding phase-phase and phase-amplitude transfer curves in traditional and new models respectively.

To verify the analyzed phase and amplitude transfer characteristics in both traditional and new two-wave models, we inject a CW light with a modulation phase range of $(-\pi, \pi)$ as the all-phase signal instead of the QPSK signal into their corresponding setups. The input and output constellations in Fig. 4(a) intuitively illustrate the regeneration characteristics in the two models. As the details shown in Figs. 4(b) and 4(c), both traditional and new models present the characteristic of phase squeezing at the four phase points of QPSK, while the corresponding amplitude characteristics at these phase points are inverse. The former will lengthen the amplitude of ASE noise due to being at the maximum $\sqrt{2}$ of amplitude gain, then the phase-dependent amplitude noise is thus formed. The latter model will squeeze the amplitude noise because of being at the minimum $\sqrt{2}/2$ of amplitude gain, then the simultaneous regeneration characteristic is obtained. Moreover, the traditional model tends to have a stronger phase regeneration ability due to the wider phase regeneration plateaus than new model. Finally, for both models, their regeneration abilities are also related to the input signal quality.

The input-output QPSK constellations obtained from the traditional, new, and three-wave models with two different input OSNRs of 8dB and 16dB respectively are all shown in Fig. 5. The regeneration factor is defined as the

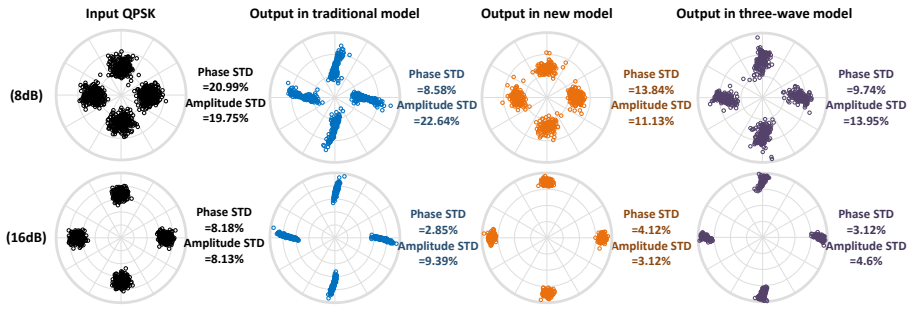

Figure 5: Input-output constellations for three kinds of models corresponding to the low (8dB) and high (16dB) quality of input QPSK signal respectively.

ratio of input noise standard deviation (STD) to output noise standard deviation. In the case of low QPSK quality (8dB), the traditional model displays a strong phase squeezing ability with a phase regeneration factor of 3.9dB and induced phase-dependent amplitude noise with an amplitude regeneration factor of -0.6dB. The new model shows simultaneous and relatively comparable phase and amplitude regeneration ability with the regeneration factors of 1.8dB and 2.5dB respectively. The three-wave model has a greater phase regeneration ability than amplitude with the regeneration factors of 3.1dB and 1.5dB respectively. As for the case with high quality of QPSK (16dB), the phase and amplitude regeneration factors for the traditional model are 4.6dB and -0.6dB respectively. They are 3dB and 4.2dB respectively in the new model, and 4dB and 2.4dB respectively in the three-wave model.

To further compare the regeneration characteristics of these three models, different input quality ranging from 6dB to 18dB is investigated and shown in Fig. 6(a). Among them, the traditional model has the strongest phase regeneration ability and worst amplitude characteristic with the regeneration factor of -0.6dB. In the new model, the simultaneous regeneration ability always exists even when the input quality is as low as 6dB, which is corresponding to the FEC threshold as calculated in Fig. 2. As for the three-wave model, it shows a greater regeneration ability in phase than in amplitude since it is the combination of traditional model and new model. Compared with the two classic

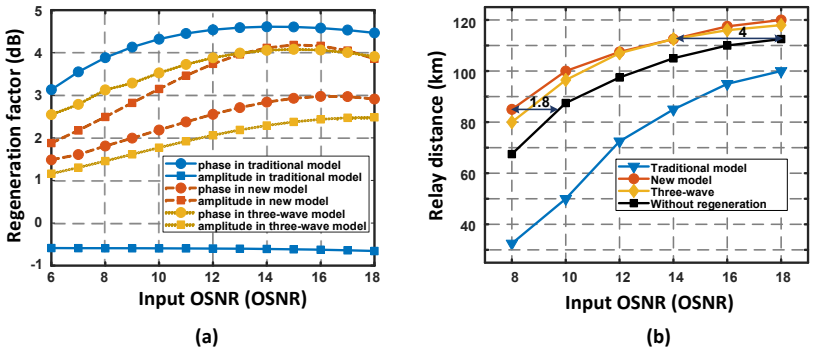

Figure 6: (a) The comparison of phase and amplitude regeneration factors versus different input OSNR in three kinds of regeneration models; (b) The comparison of relay performance versus different input OSNR at the BER of 3.8×10^{-3} in three kinds of regeneration models.

models, the new model has the most comparable ability in phase and amplitude regeneration as analyzed before.

Fig. 6(b) displays the relay performance by measuring transmission reach corresponding to the BER of 3.8×10^{-3} after the regeneration setup. The QPSK signal without regeneration is also given for reference. The results show that, in the link environment mainly affected by ASE noise, the traditional model may not be suitable to regenerate the MPSK signal due to the inherent phase-dependent amplitude noise conversion. The new model and the three-wave model could be more desired benefited from the characteristic of simultaneous amplitude and phase regeneration. More specifically, the more amplitude noise the regenerated signal has in Fig. 6(a), the more obvious conversion from amplitude noise to phase noise there will be after transmission fiber, and the shorter relay distance the regenerated signal can reach at the BER of 3.8×10^{-3} as shown in Fig 6(b). Compared with the three-wave model, the new scheme has greater advantages because of its simple implementation with one (M+1)th harmonic and slightly better relay performance, which is consistent with the analysis of optimal model. Finally, compared with the no-regeneration case, after the same transmission distance, 1.8dB OSNR improvement at the input quality of 8dB and 4dB OSNR improvement at the input quality of 14dB can

be observed in new model.

5. Conclusion

An optimal PSA model based on two-wave interference is proposed to regenerate the MPSK signal degraded by ASE noise. The new model can realize simultaneous amplitude and phase regeneration, and the regeneration ability becomes stronger with the improvement of the signal quality. The theoretical OSNR thresholds for the regeneration of different MPSK formats are very comparable with their OSNRs on FEC threshold, which can be verified by the QPSK regeneration setup. Meanwhile, the traditional model and three-wave model are also studied for reference in both theory and performance. The relay performance shows that the traditional model is not suitable for MPSK signals with ASE noise due to the phase-dependent amplitude noise conversion. Three-wave model only shows a slightly worse relay performance but with increasing system complexity. In general, the new regeneration model is specifically targeted at ASE-noise MPSK signals, and it has optimal relay performance with simple implement, which is more promising to realize all-optical relay in large-capacity, low-latency, and high-efficiency flexible optical transport networks.

Funding

National Key Research and Development Program of China (No. 2019YFB1803601), National Natural Science Foundation of China (No. 61771073), BUPT Excellent Ph.D Students Foundation (CX2019216).

References

[1] Y. Ji, J. Zhang, Y. Xiao, Z. Liu, 5G flexible optical transport networks with large-capacity, low-latency and high-efficiency, China Communications 16 (5) (2019) 19–32.

[2] Y. Ji, R. Gu, Z. Yang, J. Li, H. Li, M. Zhang, Artificial intelligence-driven autonomous optical networks: 3s architecture and key technologies, Science China Information Sciences 63 (6) (2020) 160301.

[3] X. Zhou, J. Yu, Multi-level, multi-dimensional coding for high-speed and high-spectral-efficiency optical transmission, J. Lightwave Technol. 27 (16) (2009) 3641–3653.

[4] Y. Ji, H. Wang, J. Cui, M. Yu, Z. Yang, L. Bai, All-optical signal processing technologies in flexible optical networks, Photonic Network Communications 38 (1) (2019) 14–36.

[5] X. Liu, A. R. Chraplyvy, P. J. Winzer, R. W. Tkach, S. Chandrasekhar, Phase-conjugated twin waves for communication beyond the kerr nonlinearity limit, Nature Photon 7 (7) (2013) 560–568.

[6] S. T. Le, M. E. McCarthy, N. M. Suibhne, A. D. Ellis, S. K. Turitsyn, Phase-conjugated pilots for fibre nonlinearity compensation in CO-OFDM transmission, Journal of Lightwave Technology 33 (7) (2015) 1308–1314.

[7] T. Yoshida, T. Sugihara, K. Ishida, T. Mizuochi, Spectrally-efficient dual phase-conjugate twin waves with orthogonally multiplexed quadrature pulse-shaped signals, in: OFC 2014, 2014, pp. 1–3.

[8] S. Yoshima, Y. Sun, K. R. H. Bottrill, F. Parmigiani, P. Petropoulos, D. J. Richardson, Nonlinearity mitigation through optical phase conjugation in a deployed fibre link with full bandwidth utilization, in: 2015 European Conference on Optical Communication (ECOC), 2015, pp. 1–3.

[9] G. Saavedra, Y. Sun, K. R. H. Bottrill, L. Galdino, F. Parmigiani, Z. Liu, D. J. Richardson, P. Petropoulos, R. I. Killey, P. Bayvel, Optical phase conjugation in installed optical networks, in: Optical Fiber Communication Conference, Optical Society of America, 2018, p. W3E.2.

[10] C. Sánchez, M. McCarthy, A. Ellis, P. Wright, A. Lord, Optical-phase conjugation nonlinearity compensation in flexi-grid optical networks, in:

V. Mladenov, E. Giacoumidis, J. Wei (Eds.), Recent advances on systems, signals, control, communications and computers, Recent advances in electrical engineering, WSEAS, 2015, pp. 39–43.

[11] P. Guan, F. Da Ros, M. Lillieholm, N.-K. Kjøller, H. Hu, et al, Scalable WDM phase regeneration in a single phase-sensitive amplifier through optical time lenses, Nature Communications 9 (2018) 1049.

[12] R. Slavík, F. Parmigiani, J. Kakande, C. Lundström, M. Sjödin, et al, All-optical phase and amplitude regenerator for next-generation telecommunications systems, Nature Photonics 4 (10) (2010) 690–695.

[13] J. Kakande, R. Slavík, F. Parmigiani, A. Bogris, D. Syvridis, et al, Multilevel quantization of optical phase in a novel coherent parametric mixer architecture, Nature Photonics 5 (12) (2011) 748–752.

[14] K. R. H. Bottrill, G. Hesketh, F. Parmigiani, P. Horak, D. J. Richardson, P. Petropoulos, An optical phase quantiser exhibiting suppressed phase dependent gain variation, in: Optical Fiber Communication Conference, Optical Society of America, 2014, p. W3F.7.

[15] T. Kurosu, H. N. Tan, K. Solis-Trapala, S. Namiki, Signal phase regeneration through multiple wave coherent addition enabled by hybrid optical phase squeezer, Opt. Express 23 (21) (2015) 27920–27930.

[16] G. Hesketh, P. Horak, Reducing bit-error rate with optical phase regeneration in multilevel modulation formats, Opt. Lett. 38 (24) (2013) 5357–5360. URL http://ol.osa.org/abstract.cfm?URI=ol-38-24-5357

[17] A. Mohajerin-Ariaei, M. Ziyadi, M. R. Chitgarha, A. Almaiman, Y. Cao, et al, Phase noise mitigation of qpsk signal utilizing phase-locked multiplexing of signal harmonics and amplitude saturation, Opt. Lett. 40 (14) (2015) 3328–3331.

[18] K. R. H. Bottrill, G. Hesketh, L. Jones, F. Parmigiani, D. J. Richardson, P. Petropoulos, Full quadrature regeneration of QPSK signals using sequen-

tial phase sensitive amplification and parametric saturation, Opt. Express 25 (2) (2017) 696–705.

[19] Z. Xing, H. Wang, Y. Ji, QPSK signal regeneration based on vector phase sensitive amplification with low pump powers, IEEE Access 7 (2019) 63936–63943.

[20] J. Cui, H. Wang, G.-W. Lu, L. Bai, Y. Tan, T. Sakamoto, N. Yamamoto, Y. Ji, Reconfigurable optical network intermediate node with full-quadrature regeneration and format conversion capacity, J. Lightwave Technol. 36 (20) (2018) 4691–4700.

[21] H. Wang, L. Pan, F. Lu, G. S. Murugan, Y. Sun, Y. Ji, All-optical multilevel phase quantization based on phase-sensitive amplification with low-order harmonics, J. Lightwave Technol. 36 (24) (2018) 5833–5840.

[22] T. Roethlingshoefer, G. Onishchukov, B. Schmauss, G. Leuchs, Multilevel amplitude and phase regeneration in a nonlinear amplifying loop mirror with a phase-sensitive amplifier, in: European Conference and Exhibition on Optical Communication, Optical Society of America, 2012, p. Tu.1.A.3.

[23] T. Roethlingshoefer, G. Onishchukov, B. Schmauss, G. Leuchs, All-optical simultaneous multilevel amplitude and phase regeneration, IEEE Photonics Technology Letters 26 (6) (2014) 556–559.

[24] R. Essiambre, G. Kramer, P. J. Winzer, G. J. Foschini, B. Goebel, Capacity limits of optical fiber networks, Journal of Lightwave Technology 28 (4) (2010) 662–701.

[25] R. Slavík, J. Kakande, D. J. Richardson, Practical issues and some lessons learned from realization of phase sensitive parametric regenerators, in: Optical Fiber Communication Conference, Optical Society of America, 2012, p. OW3C.4.

[26] A. D. Ellis, S. Sygletos, Phase sensitive signal processing using Semiconductor Optical Amplifiers, in: Optical Fiber Communication Confer-

ence/National Fiber Optic Engineers Conference 2013, Optical Society of America, 2013, p. OW4C.1.